

## Supplementary Material

### 3-cyanocarbazole/phosphine oxide hybrid host with increased molecular polarity towards universally enhanced efficiency for TADF OLEDs

Mengyuan Zhu,<sup>a</sup> Weiyang Hu,<sup>a</sup> Wei Shi,<sup>\*a</sup> Wenbo Yuan,<sup>a</sup> Changsheng Shi,<sup>\*b</sup> Ning Sun, and Youtian Tao<sup>\*a</sup>

<sup>a</sup> Key Laboratory of Flexible Electronics & Institute of Advanced Materials, Nanjing Tech University, Nanjing, P. R. China. E-mail address: iamwshi@njtech.edu.cn; iamyttao@njtech.edu.cn

<sup>b</sup> Department of Physics, Center for Optoelectronics Engineering Research, Yunnan University, Kunming 650091, China. E-mail address: csshi@ynu.edu.cn

#### Experimental section

##### Materials

All the reagents were purchased from Energy Chemical Co. and Sinopharm Chemical Reagent Co. without further purification. All the solvents were used as received from Nanjing WANQING chemical Glass ware & Instrument Co. and J&K Scientific.

##### General procedures

<sup>1</sup>H NMR spectra were recorded on a Bruker DMX-500 spectrometer in deuteriochloroform using tetramethylsilane (TMS;  $\delta = 0$  ppm) as an internal standard. Mass spectra were recorded using a Bruker Autoflex matrix assisted laser desorption/ionization time-of-flight (MALDI-TOF). Elemental analyses (EA) of C, H, N, and S were performed on a Vario EL III microanalyzer. Absorption spectra: Ultraviolet-visible (UV-Vis) absorption spectra of solution in dichloromethane and thin film on a quartz substrate were measured using Shimadzu UV-2500 recording spectrophotometer, and the photoluminescence (PL) spectra were recorded using a Hitachi F-4600 fluorescence spectrophotometer. Thermal gravimetric analysis (TGA) was undertaken with a METTLER TOLEDO TGA instrument. The thermal stability of the samples was determined by measuring their weight loss at a heating rate of  $10^{\circ}\text{C min}^{-1}$  from 25 to  $600^{\circ}\text{C}$  using 3 mg sample under a nitrogen atmosphere. Cyclic voltammetry (CV): The electrochemical cyclic voltammetry was conducted on a CHI voltammetric analyzer, in a  $0.1 \text{ mol L}^{-1}$  acetonitrile solution of tetrabutylammonium hexafluorophosphate ( $n\text{-Bu}_4\text{NPF}_6$ ) at a potential scan rate of  $100 \text{ mV s}^{-1}$ . The conventional three electrode configuration consists of a platinum working electrode, a platinum wire counter electrode, and an Ag/AgCl wire pseudo-reference electrode. The polymer sample was coated on the platinum sheet of working electrode. The reference electrode was checked versus ferrocenium-ferrocene ( $\text{Fc}^+/\text{Fc}$ ) as internal standard as recommended by IUPAC (the vacuum energy level: 24.8 eV). All the solutions were deaerated by bubbling nitrogen gas for a few minutes prior to the electrochemical measurements. HOMO energy levels were calculated from the equation of  $E_{\text{HOMO}} = -(E_{\text{onset}}(\text{ox}) + 4.8) \text{ eV}$ , and LUMO energy levels were deduced from the optical band gap ( $E_g$ ) values and HOMO levels.

##### OLED fabrication and measurements

The electroluminescent devices were fabricated by vacuum deposition technology, and all functional layers were fabricated on pre-treated indium tin oxide (ITO) substrates. ITO glass substrates were successively cleaned by ultrasonic wave with detergent, alcohol, acetone and deionized water, then dried at  $120^{\circ}\text{C}$  in a vacuum oven for more than 60 min. The structure of the TADF device was ITO/HAT-CN (3 nm)/TAPC (40 nm)/TCTA (5 nm)/mCP (5 nm)/EML (20 nm)/TmPyPB (40 nm)/Liq (1 nm)/Al (100 nm). Firstly, 3 nm of 1,4,5,8,9,11-

hexaazatriphenylenehexacarbonitrile (HAT-CN) was deposited on ITO substrates as hole injection layer, followed by 45 nm of 4,4'-cyclohexylidenebis[*N,N*-bis(4-methylphenyl)aniline] (TAPC) used as hole transport layer. 5 nm of tris(4-(9H-carbazol-9-yl)phenyl)amine (TCTA) and 5 nm of 1,3-di(9H-carbazol-9-yl)benzene (mCP) were used as the buffer layer to reduce hole-injection barrier from TAPC to the host in emissive layers. 20 nm of emitting layer containing host doped with emitters was deposited on the films mentioned above. Finally, the electron transport layer was 1,3,5-tri(m-pyrid-3-ylphenyl)benzene (TmPyPB) for 40 nm, meanwhile, the 1 nm of Liq and hundred-nanometer of Al were considered as the cathode layers. Current density-voltage-luminance (*J-V-L*) characteristics were tested through using a Keithley source measurement unit (Keithley 2400 and Keithley 2000) and a calibrated silicon photodiode. In addition, the EL spectra were measured by a Spectrascan PR650 spectrophotometer. It should be noted that the measurements were carried out at room temperature under ambient condition.

### Computational details

The ground-state geometries were optimized with Gaussian 09 program package using the B3LYP (Becke three parameters hybrid functional with Lee-Yang-Perdew correlation) functional and 6-31G(d) basis set.<sup>1-2</sup>

### Analyses of rate constants

The rate constants were analyzed according to the literature method with the assumption that  $k_{\text{RISC}} \gg k_{\text{r}}^{\text{T}} + k_{\text{nr}}^{\text{T}}$ , i.e. almost complete harvesting of triplet excitons to singlets. The rate constant of fluorescent radiative decay from  $S_1$  to  $S_0$  states ( $k_{\text{F}}$ ), the rate constant of the ISC, the rate constant of RISC, the rate constant of IC and the rate constant of triplet non-radiative decay ( $k_{\text{nr}}^{\text{T}}$ ) can be obtained:<sup>3-4</sup>

$$k_{\text{F}} = \frac{\Phi_{\text{P}}}{\tau_{\text{P}}} \quad (1)$$

$$\Phi_{\text{ISC}} = 1 - \Phi_{\text{P}} \quad (2)$$

$$\Phi_{\text{P}} = \frac{k_{\text{F}}}{k_{\text{F}} + k_{\text{ISC}}} \quad (3)$$

$$k_{\text{RISC}} = \frac{k_{\text{p}}k_{\text{d}}\Phi_{\text{d}}}{k_{\text{ISC}}\Phi_{\text{P}}} \quad (4)$$

$$\Phi = \frac{k_{\text{F}}}{k_{\text{F}} + k_{\text{IC}}} \quad (5)$$

$$k_{\text{nr}}^{\text{T}} = k_{\text{d}} - \left(1 - \frac{k_{\text{ISC}}}{k_{\text{F}} + k_{\text{ISC}}}\right)k_{\text{RISC}} \quad (6)$$

Where  $k_{\text{p}}$  and  $k_{\text{d}}$  represent the decay rate constant of prompt and delayed fluorescence ( $k_{\text{p}} = \frac{1}{\tau_{\text{p}}}$ ,  $k_{\text{d}} = \frac{1}{\tau_{\text{d}}}$ ), respectively.  $\Phi_{\text{p}}$  and  $\Phi_{\text{d}}$  represent quantum yields for the prompt and delayed fluorescence components. All the above parameters can be experimentally determined from typical and transient PL characteristics.

### Synthesis of compounds

The synthesis of 3FPO

tris(4-fluorophenyl) phosphine (2 g, 7.32 mmol) in dichloromethane (20 mL) and hydrogen peroxide (5 mL) was stirred at room temperature for 12h. The organic layer was separated and washed with water and dichloromethane. The extract was evaporated to dryness and then used for the next reaction without further purification.

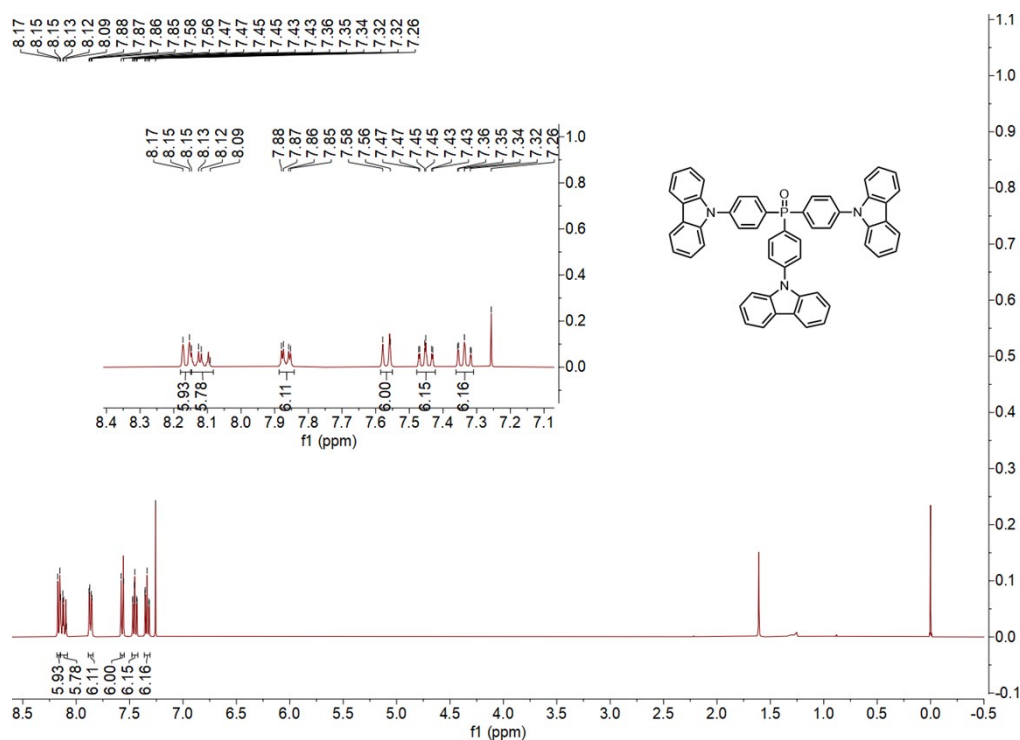
The synthesis of 3CzPO

A mixture of 3FPO (0.50 g, 1.50 mmol), 9H-carbazole (1.01 g, 6.02 mmol) and  $\text{K}_2\text{CO}_3$  (2.50 g, 18.06 mmol) in dimethyl sulfoxide (DMSO) (30 mL) was stirred at 150°C for 12 h under an  $\text{N}_2$  atmosphere. After cooling to room temperature, the mixture was poured into water, filtered, and then purified by column chromatography over

silica gel with dichloromethane/petroleum ether as the eluent to afford a white solid (Yield: 85%).  $^1\text{H-NMR}$  (400 MHz,  $\text{CDCl}_3$ )  $\delta$  ppm: 8.16 (d,  $J = 8$  Hz, 6H), 8.12 (dd,  $J_1 = 8$  Hz,  $J_2 = 12$  Hz, 6H), 7.87 (dd,  $J_1 = 8$  Hz,  $J_2 = 4$  Hz, 6H), 7.57 (d,  $J = 8$  Hz, 6H), 7.48-7.42 (m, 6H), 7.36-7.31 (m, 6H).  $^{13}\text{C-NMR}$  (100 MHz,  $\text{CDCl}_3$ )  $\delta$  ppm: 141.90, 140.25, 134.08, 131.16, 130.11, 126.99, 126.38, 124.01, 120.87, 120.65. MALDI-TOF ( $m/z$ ): calcd. for  $\text{C}_{54}\text{H}_{36}\text{N}_3\text{OP}$ : 773.26; found: 772.75. Anal. calcd. for  $\text{C}_{54}\text{H}_{36}\text{N}_3\text{OP}$ : C 83.81, H 4.69, N 5.43; found: C 83.49, H 4.21, N 5.33.

### The synthesis of 3CNCzPO

The synthetic process of 3CNCzPO was similar to that for 3CzPO as white powder with a yield of 75%.  $^1\text{H-NMR}$  (400 MHz,  $\text{CDCl}_3$ )  $\delta$  ppm: 8.48 (d,  $J = 4$  Hz, 3H), 8.20-8.14 (m,  $J_1 = 4$  Hz,  $J_2 = 8$  Hz, 6H), 7.85 (dd,  $J_1 = 4$  Hz,  $J_2 = 8$  Hz, 6H), 7.69 (dd,  $J_1 = 4$  Hz,  $J_2 = 8$  Hz, 6H), 7.57-7.53 (m, 9H), 7.46-7.41 (m, 3H).  $^{13}\text{C-NMR}$  (100 MHz,  $\text{CDCl}_3$ )  $\delta$  ppm: 141.96, 140.98, 140.82, 134.30, 132.17, 131.12, 129.62, 127.88, 127.32, 125.58, 124.21, 122.77, 122.19, 121.12, 120.10, 110.51, 103.83. MALDI-TOF ( $m/z$ ): calcd. for  $\text{C}_{57}\text{H}_{33}\text{N}_6\text{OP}$ : 848.91; found: 848.75. Anal. calcd. for  $\text{C}_{57}\text{H}_{33}\text{N}_6\text{OP}$ : C 80.65, H 3.92, N 9.90; found: C 80.51, H 3.63, N 9.90.



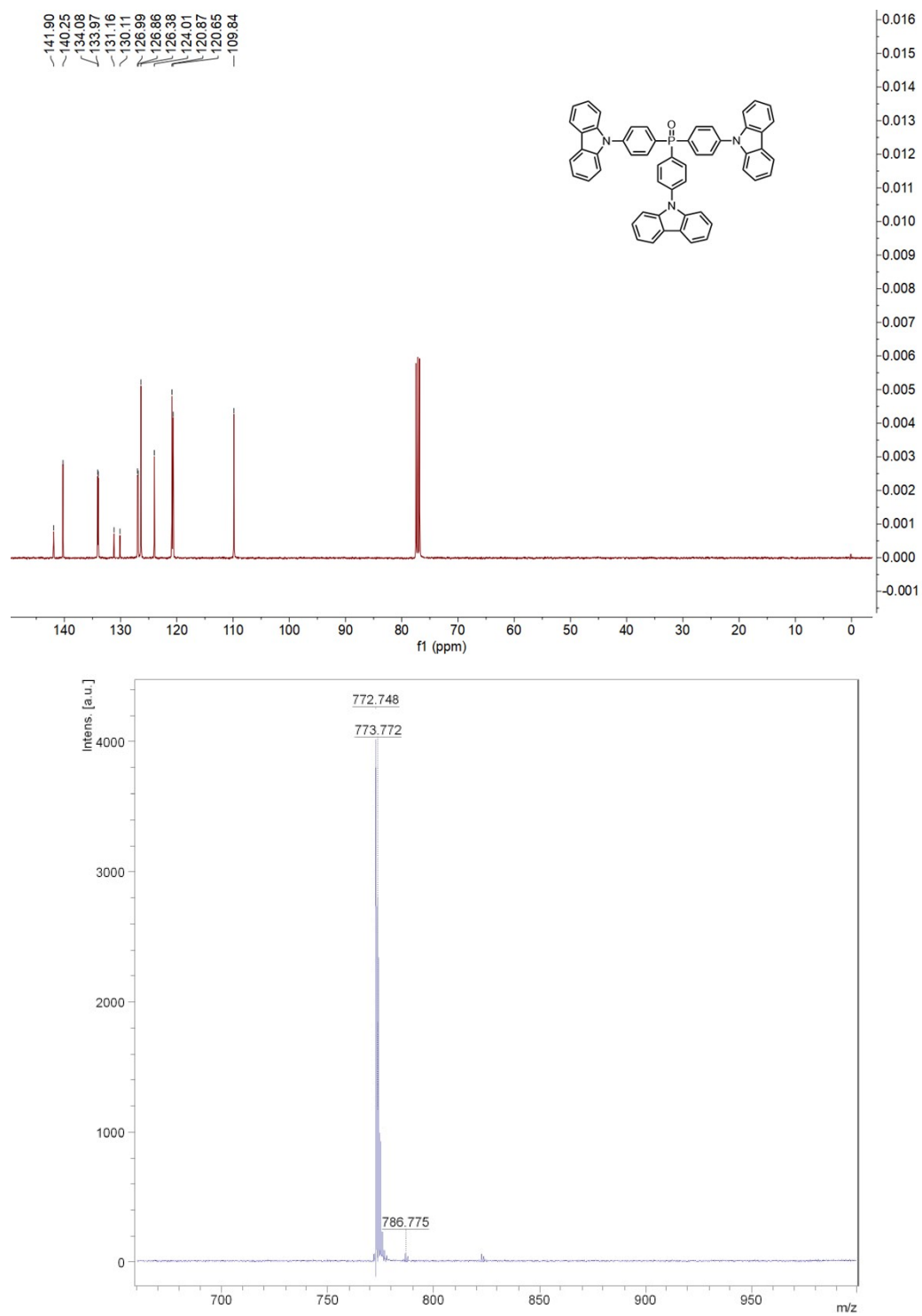
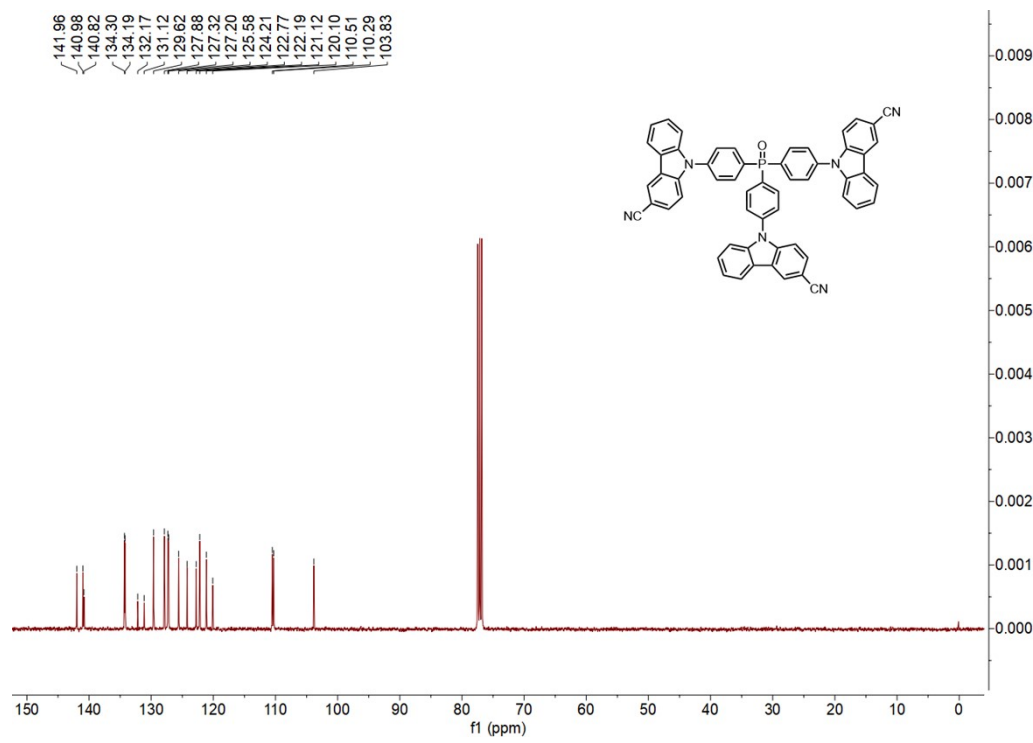
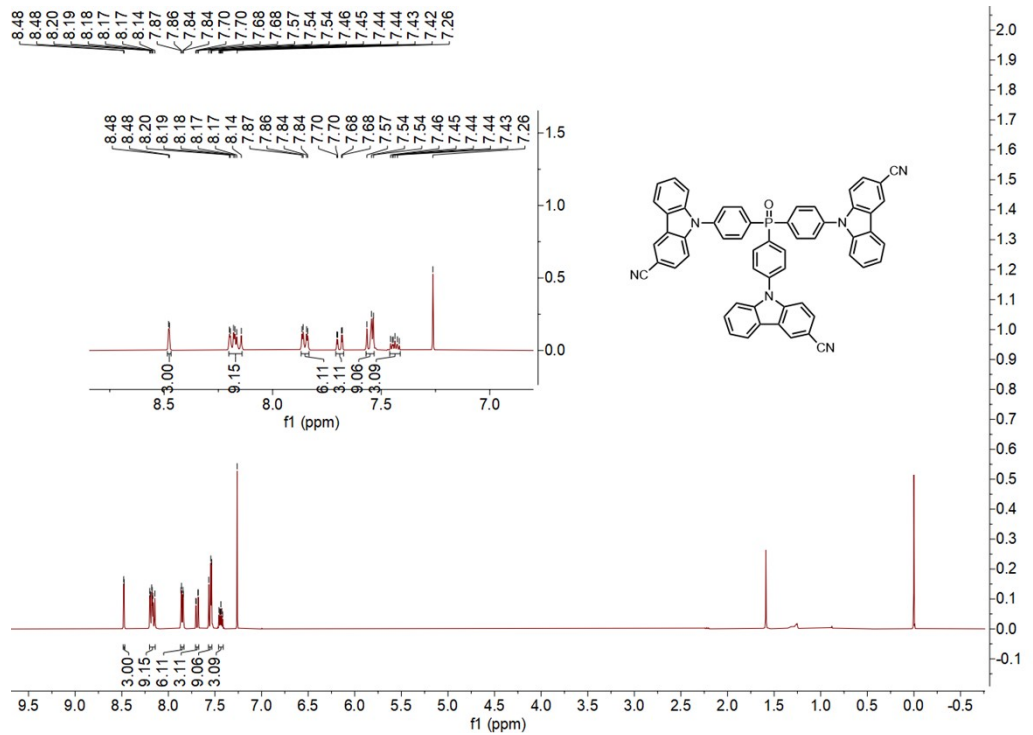


Fig. S1. <sup>1</sup>H NMR spectra, <sup>13</sup>C NMR spectra and mass spectrometry of the target compound 3CzPO.



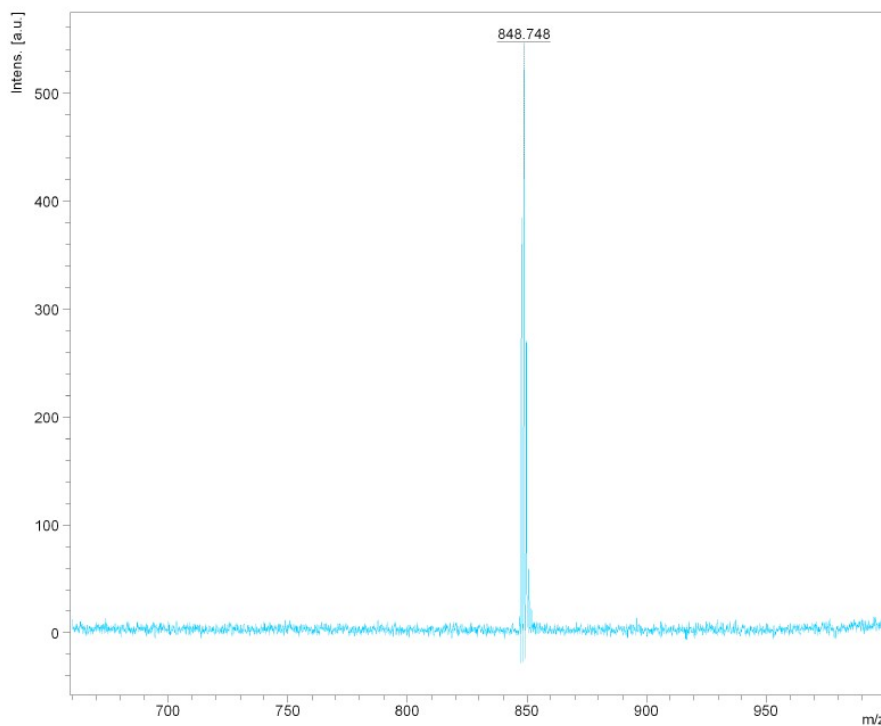


Fig. S2.  $^1\text{H}$  NMR spectra,  $^{13}\text{C}$  NMR spectra and mass spectrometry of the target compound 3CNCzPO.

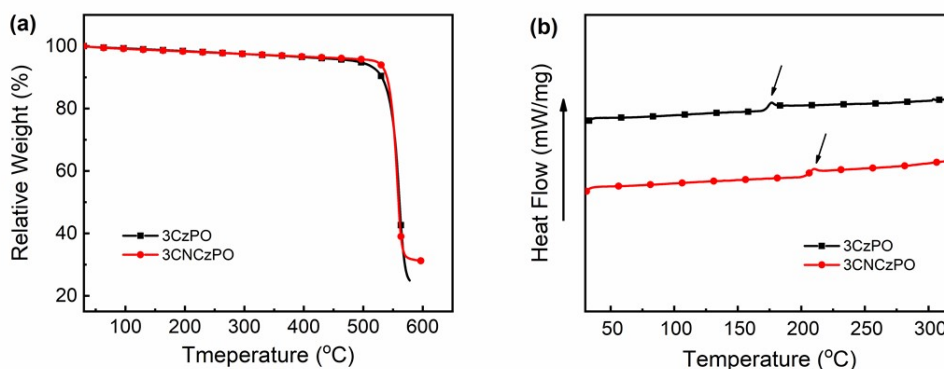


Fig. S3. (a) TGA and (b) DSC curves for Compounds 3CzPO and 3CNCzPO.

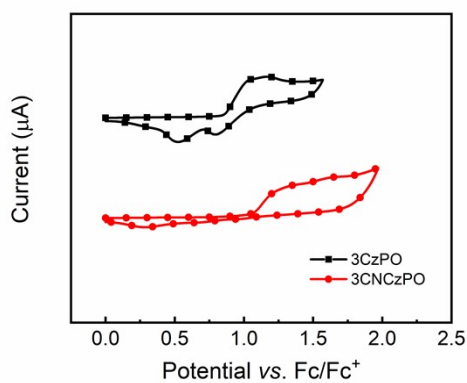


Fig. S4. Cyclic voltammograms of the compounds in  $\text{CH}_2\text{Cl}_2$  for oxidation scan.

Table S1. Photophysical rate constants of the doped films.

Doped films	3CzPO- dCF <sub>3</sub> 5tCzOXD	3CNCzPO- dCF <sub>3</sub> 5tCzOXD	3CzPO- 5tCzOXD	3CNCzPO- 5tCzOXD	3CzPO- 4tCzDOXD	3CNCzPO- 4tCzDOXD
$\Phi_{\text{PLQY}}^{[a]}$ [%]	44	32	31	27	62	51
$\Phi_{\text{p}}^{[b]}$ [%]	2.6	3.8	3.9	5.5	13.6	12.5
$\Phi_{\text{d}}^{[c]}$ [%]	41.4	28.2	27.1	21.5	48.4	38.5
$\tau_{\text{p}}^{[d]}$ [ns]	10.8	9.0	8.6	10.9	15.5	15.7
$\tau_{\text{d}}^{[e]}$ [ $\mu\text{s}$ ]	3.21	1.70	3.86	1.94	1.27	1.22
$k_{\text{p}}^{[f]}$ [ $10^7 \text{ s}^{-1}$ ]	9.3	11.1	11.0	9.1	6.4	6.4
$k_{\text{d}}^{[g]}$ [ $10^5 \text{ s}^{-1}$ ]	3.1	5.9	2.6	5.1	7.9	8.2
$k_{\text{F}}^{[h]}$ [ $10^6 \text{ s}^{-1}$ ]	2.4	4.2	4.5	5.0	8.8	8.0
$k_{\text{ISC}}^{[i]}$ [ $10^7 \text{ s}^{-1}$ ]	9.1	10.7	11.1	8.6	5.6	5.6
$k_{\text{RISC}}^{[j]}$ [ $10^6 \text{ s}^{-1}$ ]	5.1	4.6	1.8	2.1	3.2	2.9
$k_{\text{nr}}^{[k]}$ [ $10^5 \text{ s}^{-1}$ ]	1.8	4.1	1.9	3.9	3.5	4.6
$k_{\text{IC}}^{[l]}$ [ $10^6 \text{ s}^{-1}$ ]	3.0	8.9	10.2	13.7	5.4	7.6

<sup>[a]</sup> PLQY measured in doped films. <sup>[b]</sup> The prompt component of quantum yields. <sup>[c]</sup> The delayed component of quantum yields. <sup>[d]</sup> The prompt fluorescence lifetime. <sup>[e]</sup> The delayed fluorescence lifetime. <sup>[f]</sup> The decay rate constant of prompt fluorescence. <sup>[g]</sup> The decay rate constant of delayed fluorescence. <sup>[h]</sup> The rate constant of fluorescent radiative decay from  $S_1$  to  $S_0$  states. <sup>[i]</sup> The rate constant of the intersystem crossing. <sup>[j]</sup> The rate constant of the reverse intersystem crossing. <sup>[k]</sup> The rate constant of triplet non-radiative decay. <sup>[l]</sup> The rate constant of internal conversion.

## References

- 1 A. D. Becke, *Phys. Rev. A*, 1988; **38**, 3098.
- 2 C. Lee, W. Yang, and R. G. Parr, *Phys. Rev. B*, 1988, **37**, 785.
- 3 J.-X. Chen, K. Wang, C.-J. Zheng, M. Zhang, Y.-Z. Shi, S.-L. Tao, H. Lin, W. Liu, W.-W. Tao, X.-M. Ou and X.-H. Zhang, *Adv. Sci.*, 2018, **5**, 1800436.
- 4 K.-C. Pan, S.-W. Li, Y.-Y. Ho, Y.-J. Shiu, W.-L. Tsai, M. Jiao, W.-K. Lee, C.-C. Wu, C.-L. Chung, T. Chatterjee, Y.-S. Li, L.-T. Wong, H.-C. Hu, C.-C. Chen, M.-T. Lee, *Adv. Funct. Mater.*, 2016, **26**, 7560.